Precipitation Inequality Exacerbates Streamflow Inequality, but Dams Moderate it

Sai Kiran Kuntla[1], Manabendra Saharia[1,2], Samar Prakash[1], Gabriele Villarini[3,4]

[1]Department of Civil Engineering, Indian Institute of Technology Delhi, Hauz Khas, New Delhi 110016, India

[2]Yardi School of Artificial Intelligence, Indian Institute of Technology Delhi, Hauz Khas, New Delhi 110016, India

[3]Department of Civil and Environmental Engineering, Princeton University, New Jersey 08544, USA

[4]High Meadows Environmental Institute, Princeton University, New Jersey 08544, USA

Submitted for publication in *STOTEN*

Abstract

Access to clean water is a fundamental human right, yet millions worldwide face the dire consequences of water scarcity and inadequate sanitation. Water inequality, characterized by disparities in access and availability of water resources, has emerged as a critical global challenge with far-reaching social, economic, and environmental implications. Using a globally representative observational streamflow dataset and Gini coefficients, this study investigates how streamflow inequality, which has a large impact on inequality of water availability, varies spatially and temporally, and its relationship with different underlying catchment characteristics. This study finds that watersheds in arid climates exhibit a higher degree of streamflow inequality than polar and equatorial ones. Africa experiences the highest streamflow inequality, followed by Australia, while South America experiences relatively lower streamflow inequality. Around 19.6% of the catchments in Australia display an increasing trend in streamflow inequality, pointing to worsening conditions. Conversely, South America experiences a decreasing trend in streamflow inequality in 18.3% of its catchments during the same period. It is also found that a more evenly distributed precipitation within the catchment and higher dam storage capacity corresponds to more evenly distributed streamflow availability throughout the year. This study enhances our understanding of streamflow inequality worldwide, which will aid policy formulation to foster sustainable development.

Keywords: Gini coefficient, sustainable development, water, streamflow, water scarcity

1. Introduction

Surface water like rivers and lakes sustain life and enable economic activities, serving as a delicate component of the ecological balance. Access to clean and sufficient water is a fundamental human right, as recognized by the United Nations (UN General Assembly, 2010), yet vast water availability and distribution disparities persist. This inequitable distribution of water resources, compounded by factors such as population growth, climate change, and socioeconomic inequalities, has exacerbated the global water crisis (UNICEF, 2021).

Studies have shown clear regional patterns of water stress across the globe (Gassert et al., 2015; Moldsen, 2007). Water stress occurs when the demand exceeds the available amount or renewable supply. Streamflow acts as one of the major sources of water supply globally and it is important to understand its variability, which contributes to inequitable availability of water. However, there is no comprehensive global study on the temporal changes in streamflow inequality, defined as the unequal distribution of streamflow through its course, which dictates if the streamflow is the same throughout the year or concentrated during certain days. A more evenly distributed streamflow in time and improved understanding of its drivers (e.g., precipitation availability, the existence of hydraulic structures) can lead to optimal planning and utilization of water withdrawals. Moreover, understanding the geographical patterns and underlying drivers of streamflow inequality is crucial for devising effective strategies for sustainable water management. Investigating streamflow inequality globally requires a globally representative streamflow dataset and other datasets, which are not easily available. Besides, a study with a large-sample approach is expected to provide more robust insights on catchment behavior that can be widely accepted (Addor et al., 2020; Kuntla et al., 2022).

Using a globally representative streamflow dataset and other datasets such as catchment-averaged precipitation and dam storages, this study, for the first time, maps yearly streamflow inequality over a large sample of more than 5500 catchments across the globe. Such mapping provides a snapshot of the current state of streamflow inequality and serves as a powerful tool for identifying areas of critical need and informing targeted interventions. Besides, this study explores if streamflow inequality changes over time and investigates if any of the catchment's characteristics influence streamflow inequality on a yearly basis. To estimate streamflow inequality, this study employs the Gini coefficient, an established metric commonly used to measure income distribution disparities (Ceriani & Verme, 2012). Few studies have looked at precipitation inequality (Rajah et al., 2014) and global hydrological model inequality (Masaki

et al., 2014) using Gini coefficients. There is no study that utilizes observed streamflow values and Gini coefficients to map distributional patterns of streamflow. Moreover, employing this approach allows for regional comparisons, enabling the identification of regional disparities and global trends in streamflow inequality and the development of strategies towards promoting equitable water management practices.

2. Materials and methods

2.1. Data

The best available global archives are used to compute and collate variables of interest, which are described below:

a. Streamflow: The Gini coefficient values for the corresponding gauge stations are retrieved from the Global Streamflow Indices and Metadata (GSIM) archive (Gudmundsson et al., 2018). One Gini coefficient value per year describes the discharge concentration during that particular year. 1990-2013 is selected as the common time period for the analyses to maximize data availability, global spatial representativeness, and intercomparison among catchments. Based on these criteria, 5677 catchments are selected.

b. Catchment characteristics: The streamflow dataset is augmented by computing catchment-level characteristics such as Koppen-Geiger climate classes, catchment-averaged daily precipitation, number of dams in the catchment and their total storage volume, catchment-averaged Human Development Index (HDI), and the total population residing in the catchment. Koppen-Geiger aggregates climate conditions based on multiple variables and how they change with the seasons. The gridded Koppen-Geiger map produced by Kottek et al. (2006) is used in this study. It is based on average monthly temperatures and rainfall data (from 1951 to 2000) from the Climatic Research Unit (CRU) of the University of East Anglia and the Global Precipitation Climatology Centre (GPCC), respectively. Table A1 in Appendix gives the Koppen-Geiger criteria for the primary climate types. The catchment is classified based on the dominant climate, which covers more than 50 percent of the catchment area; otherwise, it is classified as “No dominant climate.” The precipitation is derived from the Multi-Source Weighted-Ensemble Precipitation (MSWEP) data (Beck et al., 2019), which is available at 0.1° resolution with global coverage. MSWEP has been used widely in previous hydrological studies (Alijanian et al., 2017; Beck et al., 2017; Xu et al., 2019). The number of dams in each catchment, their total storage volume,

and year in which these dams were built are obtained from the Global Reservoir and Dam Database (GRanD) dataset (Lehner et al., 2011). HDI is a composite index representing average achievement in key dimensions of human development: a long and healthy life, being knowledgeable, and having a decent standard of living (Kummu et al., 2018). HDI is often used by various international organizations to describe the development status of an area. More developed areas have higher HDI scores and vice versa. The average HDI in catchments is computed based on the gridded products of Kummu et al. (2018). The population in the catchment corresponding to the year 2010 is computed based on the Gridded Population of the World (GPW) dataset (CIESIN, 2016) available at a resolution of 30×30 arcsec.

2.2. Study Area

The location of the 5677 stream gauge stations is shown in Figure 1. The base map of Figure 1 corresponds to the primary Koppen-Geiger climatic classes, with Table 1 listing the number of catchments in each climate. The final gauge stations used are spatially representative across all climates and continents.

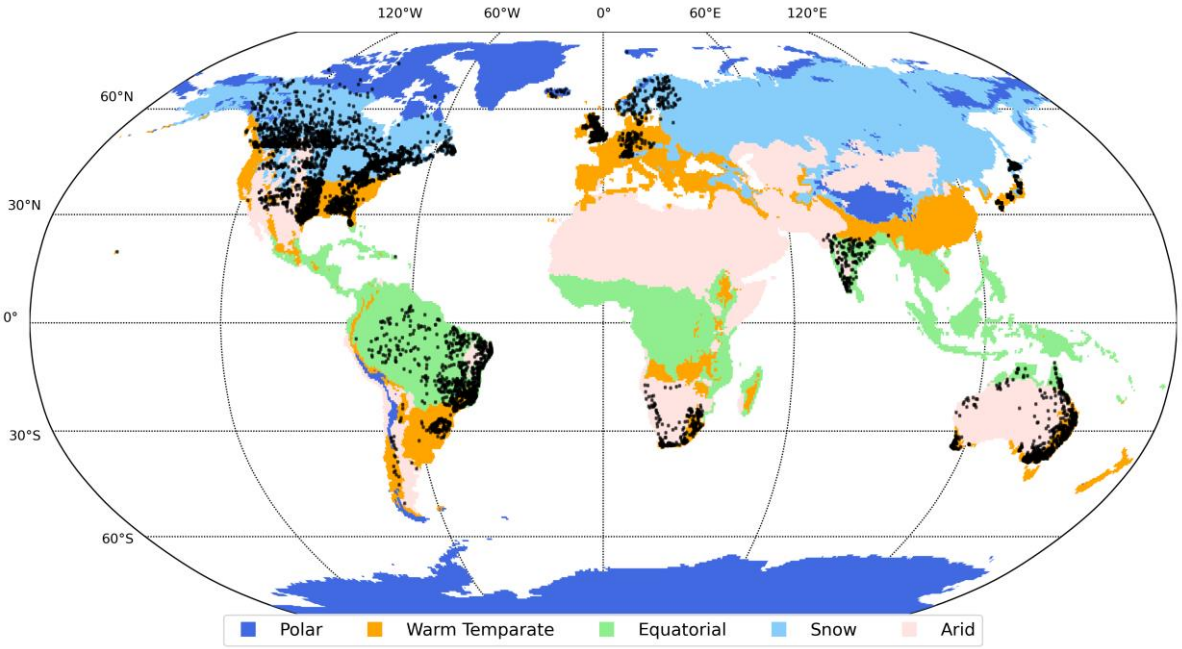

Figure 1: The spatial location of all the gauge stations and their associated climatic classes used in this study.

Table 1: Number of gauge stations in various climate regions.

Climate region	Number of gauge stations
Polar	74
Warm Temperate	2111

Equatorial	741
Snow	2257
Arid	460
No dominant class	12

2.3. Methods

This study uses the mean of the Gini coefficient of the streamflow over the study period as an indicator of global streamflow inequality. There is one Gini coefficient value per year per gauge station, and it describes the inequality of streamflow over that respective gauge station for that particular year. For daily streamflow values q of each year sorted with index i in increasing order such that $q_i \leq q_{i+1}$, GINI is defined as:

$$\text{GINI} = \frac{1}{n}\left(n+1-2\left(\frac{\sum_{i=1}^{n}(n+1-1)qi}{\sum_{i=1}^{n} qi}\right)\right) \quad \text{(Equation 1)}$$

where n is the number of daily streamflow values available for that year. The Gini coefficient ranges from 0 to 1. A value of 0 indicates a uniform distribution of flows throughout the year, whereas a value of 1 indicates that all the flows occur on a single day, with values between 0 and 1 representing intermediate cases.

In addition, this study explores the trends in the annual Gini coefficient to observe the changes in streamflow inequality over the given study period. Mann-Kendall (MK) test is a popular nonparametric test to detect monotonic trend in time series data (Kendall, 1948; Mann, 1945). To account for the potential presence of serial correlation, this study employs the Modified MK test using the trend free pre-whitening (TFPW) method (Yue et al., 2002) to evaluate the trends. The significance level was adjusted to 10% to identify potentially important trends that might possess practical significance and allow for a more explanatory approach. Furthermore, box plots are used to explore the ranges of Gini coefficient over different climates and continents.

Since precipitation is a major forcing for runoff or streamflow, the Gini coefficient for catchment-average daily precipitation is computed using Equation 1 for every year over the same time period as streamflow. Subsequently, the spatial plots of mean-precipitation Gini over the study period and the trends in annual Gini are examined, similar to what was done for streamflow, to relate the influence of precipitation on streamflow inequality. Moreover, to further investigate the relationship between streamflow and precipitation Gini across various Koppen-Geiger climatic classes, a linear regression model has been fit between streamflow

and precipitation Gini across the climates. An analysis of variance (ANOVA) has been performed on the model with a significance level of 0.05, which allows us to test the equality of regression slopes across different climates, i.e., to test whether the relationship between precipitation Gini and streamflow Gini is consistent across climates or if there are significant differences.

Finally, this study investigates the relationship between streamflow inequality (denoted by the streamflow Gini) and other exogenous variables, including the number of dams and their total volume and population in each catchment. Furthermore, to analyze how dam construction has impacted streamflow inequality over the catchments, this study examines how the average Gini has changed after dam construction. Catchments in which dams were built during the study period (1990-2013) are identified first; then, the record is split before and after the dam's construction year to compute the average streamflow Gini for the two subperiods.

3. Results

3.1. Spatial distribution and the trends in Gini coefficients of streamflow

Figure 2 presents the spatial distribution of the mean Gini coefficient between 1990 and 2013. Southwest Africa, northeastern Brazil, western India, west coast of and eastern Australia, scattered clusters across the USA have high streamflow inequality. In comparison, catchments with great equality have been scattered around Canada, central and eastern Brazil, and a few places in Europe. At the same time, to quantitively investigate streamflow inequality across all the continents, box plots are employed. As shown in the inset plot of Figure 2, Africa has more streamflow inequality, with high median and quartile values of streamflow Gini, followed by Australia. While South America, followed by Europe, has less streamflow inequality among others, with smaller median and quartile values.

A glance at Figure 2, and Figure A1 (in Appendix), reveals that inequality in streamflow is primarily consistent with inequality in precipitation. However, in a few places like Canada, central and southern United States, eastern South America, many places in Europe, and Southwestern Australia, the streamflow concentration is more equally dispersed compared to that of precipitation, which could be due to many reasons including proper streamflow management.

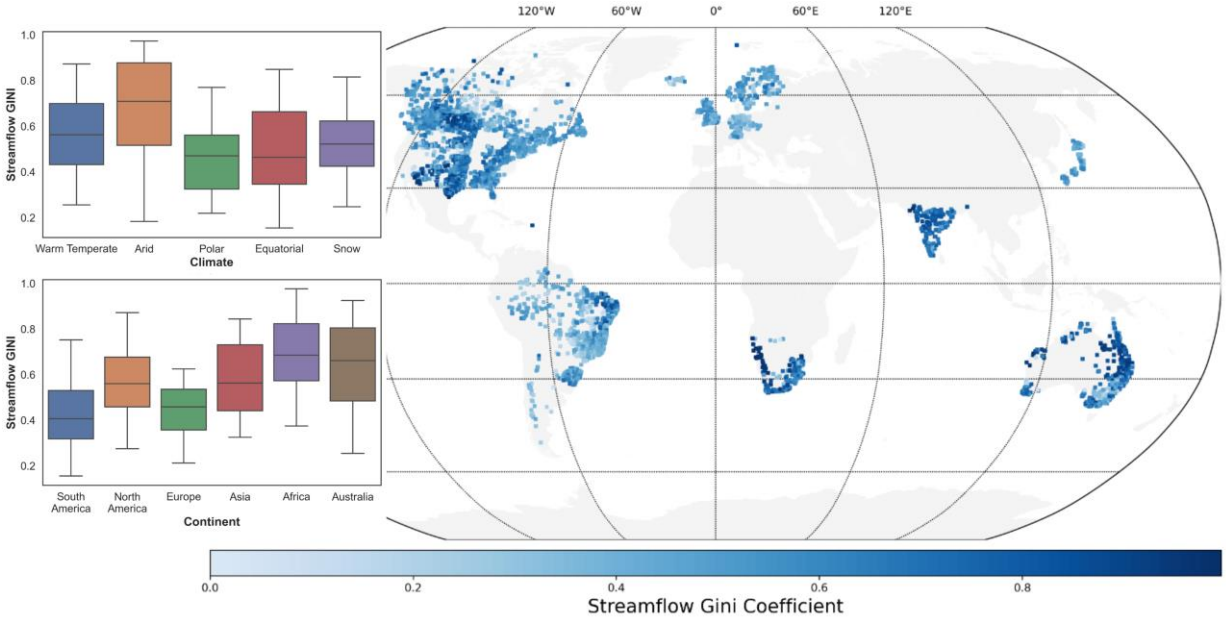

Figure 2: Spatial distribution of the mean Gini coefficient for streamflow over the corresponding stream gauge stations between 1990 and 2013. A value of 0 indicates a uniform distribution of flows throughout the year, whereas a value of 1 indicates that all the flows occur on a single day. The boxplots in the inset plot summarize the mean streamflow Gini over different climates. The box spans the interquartile range (i.e., 25th and 75th percentiles), with the bar in the middle representing the median. The whiskers are the two vertical lines outside the box extended until the 5th and 95th percentiles.

To see if the streamflow inequality is increasing or decreasing over time, the Modified Mann-Kendall trend test (Figure 3) has been performed, with the corresponding results for precipitation in Figure A2 in the Appendix. Interestingly, the trends in precipitation inequality have been observed to be not obvious across the globe, with a few clear regional clusters. At many regions the streamflow inequality trends are observed to be in line with precipitation trends. However, there has been a considerable trend in streamflow inequality across the globe spread even in regions where no trend is observed in precipitation inequality. Notably, many catchments display an increasing streamflow inequality in Australia (19.6 %). In contrast, in 18.3% of the catchments in South America, streamflow inequality is decreasing. Among climates, streamflow inequality in catchments with a Polar and Equatorial climate is decreasing by 19.2 and 17.2%, respectively, while in the Warm temperate is increasing by 14%.

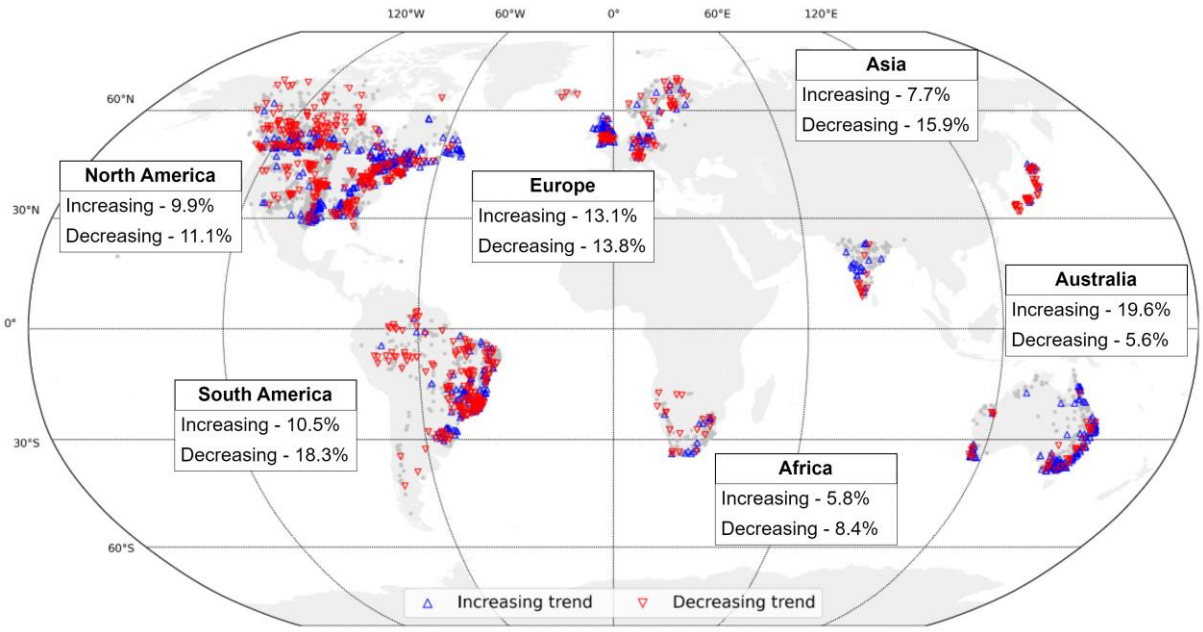

Figure 3: Trends in streamflow Gini coefficient (streamflow inequality) between 1990 and 2013 based on the Modified Mann-Kendall trend test at a 10% significance level. The inset text boxes display the percentage of stations with statistically significant decreasing and increasing trends in each continent.

Reasoning the causes of these streamflow inequality trends is beyond the scope of this study. In addition to what examined here, several factors, both natural and anthropogenic, can alter streamflow. These factors can have significant effects on the quantity, timing, and variability of water flow in a stream for both short-term and long-term. Some key factors that can alter streamflow include climate change, changes in land use, urbanization, reservoir operations, water diversions and withdrawals in the upstream, alterations to the natural features of a watershed (e.g., channel modifications, land reclamation), erosion and sedimentation, natural events like landslides, volcanic eruptions, and earthquakes by changing the landscape and redirecting watercourses, changes in vegetation, and agricultural practices, and changes in groundwater levels. Integrated watershed management approaches are often employed to address these complex issues to ensure sustainable and resilient water systems. It is important to note that many factors are interconnected, and changes in one factor can have cascading effects on streamflow.

3.2. Exploring the relationship between streamflow inequality and catchment characteristics

This study uses boxplots to further advance our understanding of the current scenario of streamflow inequality in various climates (inset of Figure 2). Streamflow inequality is high in

Arid climates, with the highest median and quartile values, as expected, followed by Warm temperate. In contrast, Equatorial and Polar climates have the lower median values.

Figure 4 shows that an increase in precipitation inequality increases streamflow inequality across all the climates. ANOVA test performed to assess the equality of regression slopes across different climates reveals that climate and precipitation Gini have a significant effect on streamflow Gini with p-values much smaller than 0.01, indicating that regions with different climates have different mean streamflow Gini values and changes in precipitation Gini significantly affect streamflow Gini. In addition, a highly statistically significant interaction between precipitation Gini and climate has been observed, suggesting that the relationship between precipitation Gini and streamflow Gini varies significantly across different climates.

At the same time, the high slope of Warm temperate in Figure 4, among others, indicates that the precipitation inequality is strongly related to streamflow inequality in these regions compared to other climates. In contrast, precipitation has the least influence on catchments in the Polar climate compared to the other climates.

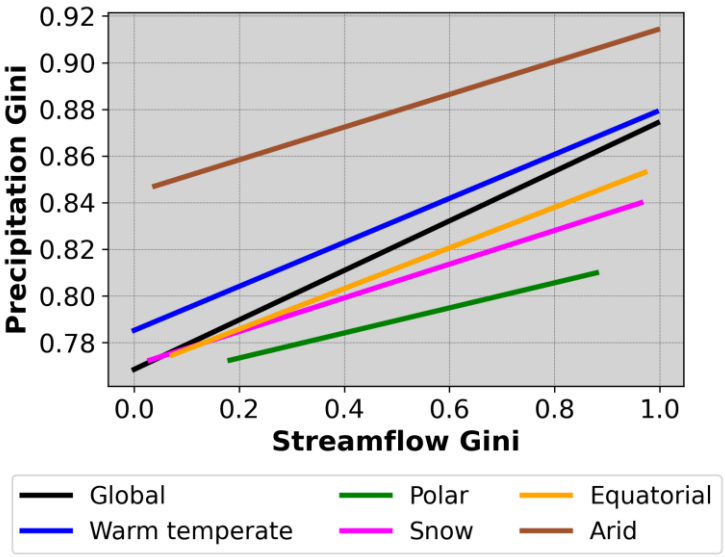

Figure 4: A straight line fit between streamflow Gini and their corresponding precipitation Gini for different climates.

Figure 5(a) shows a scatter plot between streamflow Gini and population, highlighting that there is a general tendency towards increasing streamflow inequality for decreasing population in the catchment. However, catchments with high populations but low HDI (shown by yellow hue) exhibit high streamflow inequality.

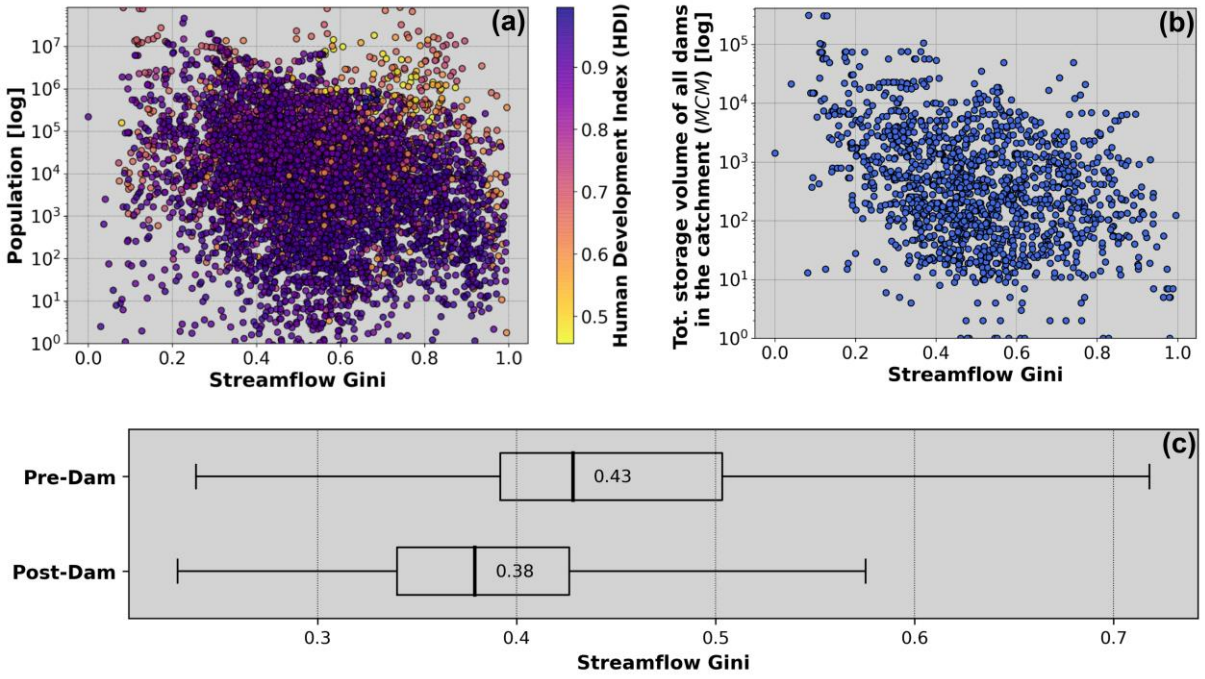

Figure 5: Scatter plot between **(a)** Streamflow Gini and Population count in the corresponding catchments across the globe. The points are color-coded by the Human Development Index (HDI, i.e., more developed areas have higher HDI scores and vice versa). **(b)** Streamflow Gini vs. Total storage volume in million cubic meters of all the dams in the respective catchment. **(c)** Box plot of streamflow Gini pre- and post-dam construction. The box spans the interquartile range (i.e., 25th and 75th percentiles), with the bar in the middle representing the median and its corresponding value as text within the box. The whiskers are the two horizontal lines outside the box extended until the 5th and 95th percentiles.

Figure 5(b) shows that the more the total storage of all the dams in the catchment, the more equality in streamflow discharge throughout the year. There is a gradual increase in streamflow inequality as dam storage decreases. At the same time, the boxplot of streamflow Gini pre- and post-dam construction further strengthens the statement that dams moderate the streamflow inequality by contributing to a more equal distribution of streamflow over the year. The median of Gini over the catchments where dams were constructed in the study period (1990-2013) reduced from 0.43 to 0.38 after the construction of the dam, with these differences that are exacerbated when we consider the upper tail of the Gini distributions. Besides, in many catchments in developing countries such as Brazil and India, where dams were constructed during the study period, there is a considerable influence on streamflow Gini (inequality). For example, the construction of Bennithora Dam in 2003 in the Krishna Basin in India has resulted in the reduction of average streamflow Gini from 0.77 to 0.69 after 2003 at Malkhed gauge station. Similarly, the construction of the Serra da Messa Dam in Brazil in the year 1998 over Tocantins River has resulted in reduced average Gini (streamflow

inequality) at the Peixe (from 0.36 to 0.22), and Miracema do Tocantins (from 0.40 to 0.35) locations. At the same time, many such dam constructions are observed in Brazil, which are included in our pre- and post-dam analysis study. Subsequently, these constructions would have resulted in decreasing streamflow inequality in Brazil, indeed in South America, as per the trend analysis carried out in this study (Figure 3).

4. Conclusions and Discussions

By applying the Gini coefficient to the streamflow domain, this study quantitatively assessed the extent of streamflow inequality, shedding light on the geographical areas disproportionately affected. Moreover, the findings of this study revealed the underlying socio-environmental factors that contribute to such inequalities. By identifying hotspots of streamflow inequality and knowing how it changes over time, policymakers, international organizations, and local communities can prioritize interventions and allocate resources to regions in dire need. The primary findings of this study are as follows:

- Southwestern Africa, northeastern Brazil, western India, the west coast of and eastern Australia, scattered clusters across the USA have high streamflow inequality. In comparison, many catchments with great equality were scattered around Canada, central and eastern Brazil, and a few places in Europe. By continent, boxplots reveal that Africa has more streamflow inequality than other regions, with high median and quartile values of streamflow Gini, followed by Australia. While South America, followed by Europe, has less streamflow inequality.
- Streamflow inequality is changing across the globe. Notably, many catchments display an increasing streamflow inequality in Australia (19.6%). In contrast, in 18.3% of the catchments in South America, streamflow inequality is decreasing. Among climates, streamflow inequality in catchments with Polar (19.2%) and Equatorial (17.2%) climate is decreasing, while increasing in the Warm temperate climate.
- Streamflow inequality is high in Arid climates, with the highest median and quartile values, followed by Warm temperate. In contrast, Equatorial and Polar climates are among the regions with the lowest median values.
- An increase in precipitation inequality increases streamflow inequality across all the climates. Catchments in the Warm temperate climate, among others, suggest

that precipitation inequality strongly relates to streamflow inequality. In comparison, catchments in Polar climates are the least influenced of precipitation on streamflow relative to catchments with other climates.

- Streamflow inequality is observed to be low where the population is high, except in catchments with low HDI.
- The more the total storage of all the dams in the catchment, the more equality in streamflow is observed throughout the year. There is a gradual decrease in streamflow inequality as the dams' storage increases. This observation has been further consolidated with a pre- and post-dam streamflow inequality analysis in catchments where dams were built in the study period.

Hopefully, this study will inspire further research, dialogue, and collaborative efforts to address the urgent issue of water inequality and pave the way for a more equitable and sustainable water future. Also, it is hoped that this study will inspire in thinking towards employing more interdisciplinary sophisticated methods in hydrology in future studies without any boundaries. At the same time, it is highlighted that though dam construction has positive aspects, as found in this study, it is imperative to meticulously assess and address the ecological, environmental, and socioeconomic impacts associated with such projects during planning and construction for the sake of sustainable development and the mitigation of adverse consequences on both the environment and society. For instance, ecologically, dams can disrupt natural flow regimes, negatively affecting aquatic ecosystems and fish habitats (Hoque et al., 2022). Environmentally, reservoir operation can either alleviate or exacerbate the impact of climate change on streamflow and flood characteristics (Yun et al., 2020). On the socioeconomic front, large dams are often found to be only marginally economically viable, with considerable cost overruns (World Commission on Dams, 2000). The construction of dams may displace communities and impact water access, potentially leading to conflicts; however, on a positive note, dams can enhance water availability for agriculture, foster economic development, and provide renewable energy, thereby contributing to improved living standards when implemented with inclusive and sustainable practices.

Acknowledgments

This research was conducted in the HydroSense Lab (https://hydrosense.iitd.ac.in/) of the Indian Institute of Technology Delhi and the authors acknowledge IIT Delhi High Performance Computing facility for providing computational and storage resources. Dr.

Manabendra Saharia gratefully acknowledges financial support for this work through an ISRO Space Technology Cell grant (Grant number: RP04139); MoES Monsoon Mission III; IC-IMPACTS (Grant number: RP04558), and the Coalition for Disaster Resilient Infrastructure (CDRI) Fellowship (Grant number: RP04569).

Compliance with Ethical Standards

The authors declare that they have no known competing financial interests or personal relationships that could have appeared to influence the work reported in this paper.

Author Contributions

SKK: Conceptualization, Methodology, Formal analysis, Data Curation, Writing - Original Draft

MS: Conceptualization, Methodology, Writing - Review & Editing

SP: Formal analysis, Data Curation

GV: Writing - Review

Data Availability

The datasets used in this study are available from the following sources:

- Global Flood characterization (GloFlo) Database: https://doi.org/10.5281/zenodo.7158028
- Global Streamflow Indices and Metadata (GSIM) archive: https://doi.org/10.1594/PANGAEA.887477
- Global Koppen-Geiger climate classification: http://koeppen-geiger.vu-wien.ac.at/present.htm
- Precipitation data from Multi-Source Weighted-Ensemble Precipitation (MSWEP).
- Dams information from Global Reservoir and Dam Database (GRanD): https://doi.org/10.7927/H4N877QK
- Population from Gridded Population of the World (GPW): https://doi.org/10.7927/H4X63JVC
- Human Development Index (HDI): https://doi.org/10.5061/dryad.dk1j0

References

Addor, N., Do, H. X., Alvarez-Garreton, C., Coxon, G., Fowler, K., & Mendoza, P. A. (2020). Large-sample hydrology: Recent progress, guidelines for new datasets and grand challenges. *Hydrological Sciences Journal*, *65*(5), 712–725. https://doi.org/10.1080/02626667.2019.1683182

Alijanian, M., Rakhshandehroo, G. R., Mishra, A. K., & Dehghani, M. (2017). Evaluation of satellite rainfall climatology using CMORPH, PERSIANN-CDR, PERSIANN, TRMM, MSWEP over Iran. *International Journal of Climatology*, *37*(14), 4896–4914. https://doi.org/10.1002/joc.5131

Beck, H. E., Vergopolan, N., Pan, M., Levizzani, V., van Dijk, A. I. J. M., Weedon, G. P., Brocca, L., Pappenberger, F., Huffman, G. J., & Wood, E. F. (2017). Global-scale evaluation of 22 precipitation datasets using gauge observations and hydrological modeling. *Hydrology and Earth System Sciences*, *21*(12), 6201–6217. https://doi.org/10.5194/hess-21-6201-2017

Beck, H. E., Wood, E. F., Pan, M., Fisher, C. K., Miralles, D. G., Dijk, A. I. J. M. van, McVicar, T. R., & Adler, R. F. (2019). MSWEP V2 Global 3-Hourly 0.1° Precipitation: Methodology and Quantitative Assessment. *Bulletin of the American Meteorological Society*, *100*(3), 473–500. https://doi.org/10.1175/BAMS-D-17-0138.1

Ceriani, L., & Verme, P. (2012). The origins of the Gini index: Extracts from Variabilità e Mutabilità (1912) by Corrado Gini. *The Journal of Economic Inequality*, *10*(3), 421–443. https://doi.org/10.1007/s10888-011-9188-x

CIESIN. (2016). *Gridded Population of the World (GPW), v4*. NASA Socioeconomic Data and Applications Center (SEDAC). https://doi.org/10.7927/H4X63JVC

Gassert, F., Reig, P., Shiao, T., Luck, M., Landis, M., Reig, P., & Shiao, T. (2015). Aqueduct Global Maps 2.1: Constructing Decision-Relevant Global Water Risk Indicators. *World Resources Institute*. https://www.wri.org/research/aqueduct-global-maps-21-indicators

Gudmundsson, L., Do, H. X., Leonard, M., & Westra, S. (2018). *The Global Streamflow Indices and Metadata Archive (GSIM) – Part 2: Quality control, time-series indices and homogeneity assessment*. 18.

Hoque, Md. M., Islam, A., & Ghosh, S. (2022). Environmental flow in the context of dams and development with special reference to the Damodar Valley Project, India: A review. *Sustainable Water Resources Management*, *8*(3), 62. https://doi.org/10.1007/s40899-022-00646-9

Kendall, M. G. (1948). *Rank correlation methods*. Griffin.

Kottek, M., Grieser, J., Beck, C., Rudolf, B., & Rubel, F. (2006). World Map of the Köppen-Geiger climate classification updated. *Meteorologische Zeitschrift*, 259–263. https://doi.org/10.1127/0941-2948/2006/0130

Kummu, M., Taka, M., & Guillaume, J. H. A. (2018). Gridded global datasets for Gross Domestic Product and Human Development Index over 1990–2015. *Scientific Data*, *5*(1), 180004. https://doi.org/10.1038/sdata.2018.4

Kuntla, S. K., Saharia, M., & Kirstetter, P. (2022). Global-scale characterization of streamflow extremes. *Journal of Hydrology*, *615*, 128668. https://doi.org/10.1016/j.jhydrol.2022.128668

Lehner, B., Liermann, C. R., Revenga, C., Vörösmarty, C., Fekete, B., Crouzet, P., Döll, P., Endejan, M., Frenken, K., & Magome, J. (2011). *Global Reservoir and Dam Database, Version 1 (GRanDv1)*. https://doi.org/10.7927/H4N877QK

Mann, H. B. (1945). Nonparametric Tests Against Trend. *Econometrica*, *13*(3), 245–259. https://doi.org/10.2307/1907187

Masaki, Y., Hanasaki, N., Takahashi, K., & Hijioka, Y. (2014). Global-scale analysis on future changes in flow regimes using Gini and Lorenz asymmetry coefficients. *Water Resources Research*, *50*(5), 4054–4078. https://doi.org/10.1002/2013WR014266

Moldsen, D. (2007). *Water for Food Water for Life: A Comprehensive Assessment of Water Management in Agriculture* (1st Edition). Routledge. https://www.routledge.com/Water-for-Food-Water-for-Life-A-Comprehensive-Assessment-of-Water-Management/Molden/p/book/9781844073962

Rajah, K., O'Leary, T., Turner, A., Petrakis, G., Leonard, M., & Westra, S. (2014). Changes to the temporal distribution of daily precipitation. *Geophysical Research Letters*, *41*(24), 8887–8894. https://doi.org/10.1002/2014GL062156

UN General Assembly. (2010). *The human right to water and sanitation: Resolution adopted by the General Assembly (A/RES/64/292)*. United Nations. https://documents-dds-ny.un.org/doc/UNDOC/GEN/N09/479/35/PDF/N0947935.pdf

UNICEF. (2021). *Reimagining WASH - Water security for all*. https://www.unicef.org/media/95241/file/water-security-for-all.pdf

World Commission on Dams (Ed.). (2000). *Dams and development: A new framework for decision-making*. Earthscan. https://archive.internationalrivers.org/sites/default/files/attached-files/world_commission_on_dams_final_report.pdf

Xu, Z., Wu, Z., He, H., Wu, X., Zhou, J., Zhang, Y., & Guo, X. (2019). Evaluating the accuracy of MSWEP V2.1 and its performance for drought monitoring over mainland China. *Atmospheric Research*, *226*, 17–31. https://doi.org/10.1016/j.atmosres.2019.04.008

Yue, S., Pilon, P., Phinney, B., & Cavadias, G. (2002). The influence of autocorrelation on the ability to detect trend in hydrological series. *Hydrological Processes*, *16*(9), 1807–1829. https://doi.org/10.1002/hyp.1095

Yun, X., Tang, Q., Wang, J., Liu, X., Zhang, Y., Lu, H., Wang, Y., Zhang, L., & Chen, D. (2020). Impacts of climate change and reservoir operation on streamflow and flood characteristics in the Lancang-Mekong River Basin. *Journal of Hydrology*, *590*, 125472. https://doi.org/10.1016/j.jhydrol.2020.125472

Appendix

Table A1: Climate formula of Koppen-Geiger for the main climates (Kottek et al., 2006). Where, T_{max} and T_{min} are the monthly mean temperatures of the warmest and coldest months, respectively. P_{ann} is the accumulated annual precipitation. $P_{th}$is a dryness threshold in mm, which depends on $\{T_{ann}\}$, the absolute measure of the annual mean temperature in °C, and on the annual cycle of precipitation: P_{th} = 2$\{T_{ann}\}$ if at least 2/3 of the annual precipitation occurs in winter; P_{th} = 2$\{T_{ann}\}$+28 if at least 2/3 of the annual precipitation occurs in summer; P_{th} = 2$\{T_{ann}\}$+14 otherwise.

Climate	Criterion
Polar	T_{max} < +10 °C
Warm Temperate	−3 °C < T_{min} < +18 °C
Equatorial	T_{min} ≥ +18 °C
Snow	T_{min} ≤ −3 °C
Arid	P_{ann} < 10 P_{th}

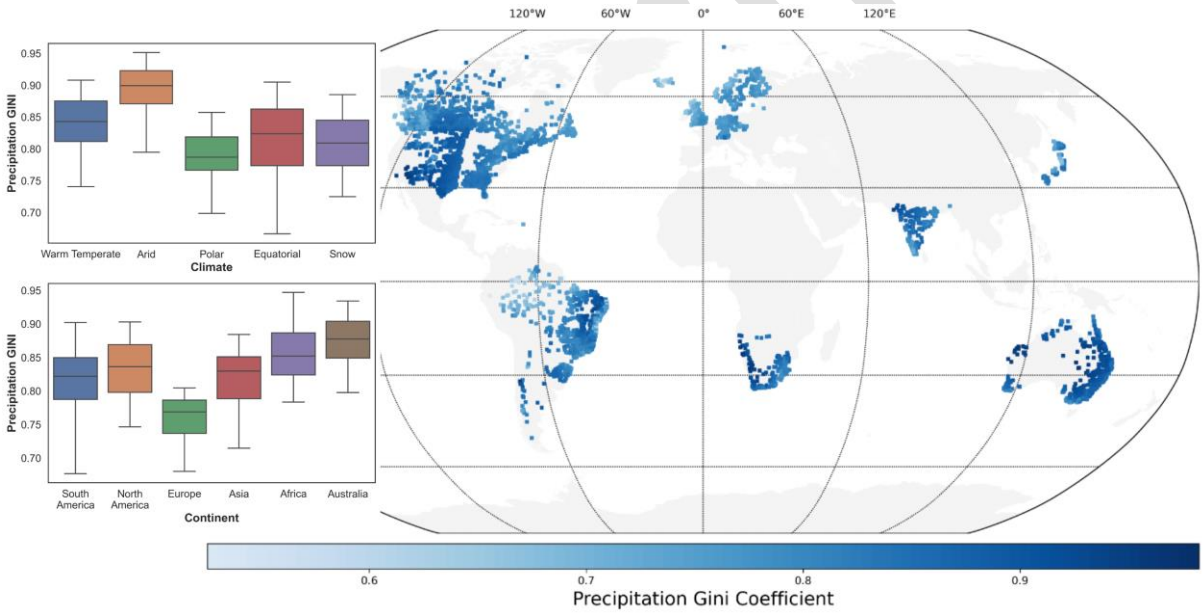

Figure A1: Spatial distribution of the mean Gini coefficient for precipitation over the catchments of corresponding stream gauge stations between 1990 and 2013. A value of 0 indicates a uniform distribution of flows throughout the year, whereas a value of 1 indicates that all the flows occur on a single day. The boxplots in the inset plot summarize the mean streamflow Gini over different climates. The box spans the interquartile range (i.e., 25th and 75th percentiles), with the bar in the middle representing the median. The whiskers are the two vertical lines outside the box extended until the observations' extremes at 5th and 95th percentiles.

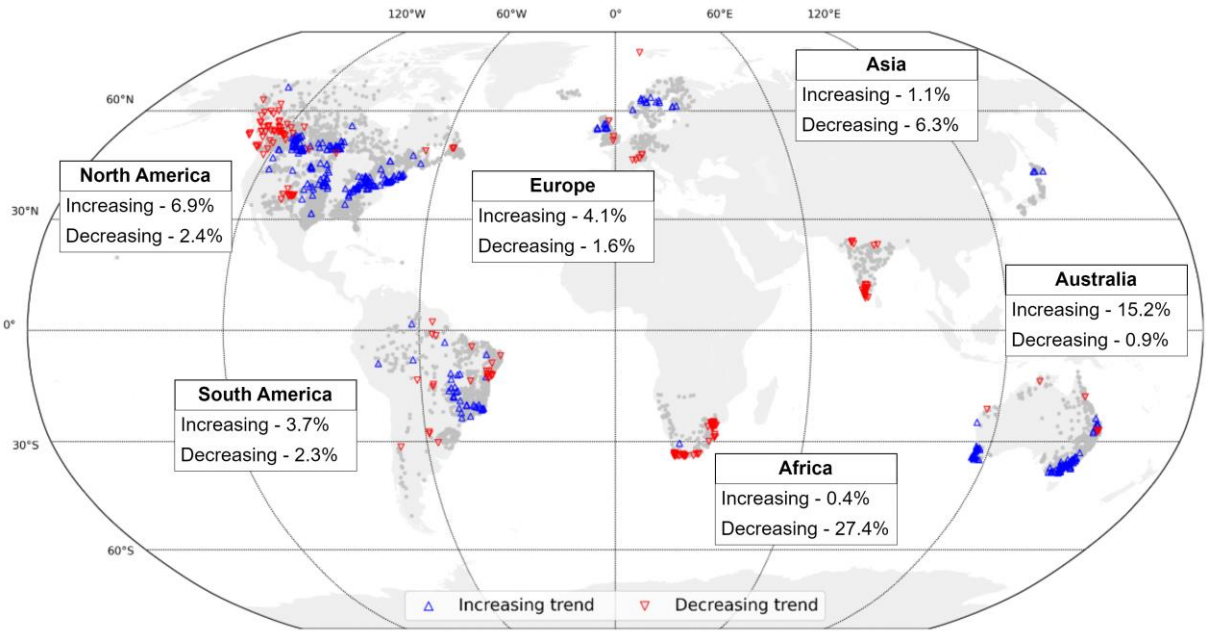

Figure A2: Trends in precipitation Gini coefficient between 1990 and 2013 based on the Modified Mann Kendall trend test at 10% significance level. The inset text boxes display the percentage of stations with statistically significant decreasing and increasing trends in each continent.